Laser-heated high-temperature NMR - a time-resolution study

Jones, Aled R.; Shaw-West, Rachel N.; Winter, Rudolf; Massiot, Dominique; Florian, Pierre; Wolff, Matthias

Published in:
Applied Magnetic Resonance

DOI:
10.1007/s00723-007-0035-y

Publication date:
2007

Citation for published version (APA):
Jones, A. R., Shaw-West, R. N., Winter, R., Massiot, D., Florian, P., & Wolff, M. (2007). Laser-heated high-temperature NMR - a time-resolution study. *Applied Magnetic Resonance*, *32*(4), 635-646. https://doi.org/10.1007/s00723-007-0035-y

Laser-heated high-temperature NMR - a time-resolution study

Rudolf Winter[1], Aled Jones[1], Rachel Shaw-West[1,#], Matthias Wolff[1,%], Pierre Florian[2], Dominique Massiot[2]

[1]Materials Physics, University of Wales Aberystwyth, Aberystwyth, Wales

[2]CNRS Centre de Recherche sur les Matériaux à Hautes Températures, Orléans, France

[#]present address: School of Physics and Astronomy, University of Birmingham, England

[%]on leave from: Pulvertechnologie, Universität des Saarlandes, Saarbrücken, Germany

Laser-heated NMR - time resolution

Dr Rudolf Winter

Materials Physics

University of Wales Aberystwyth

Penglais

Aberystwyth SY23 3BZ

Wales

ruw@aber.ac.uk

Abstract.

The time resolution achievable in *in-situ* high-temperature nuclear magnetic resonance (NMR) experiments is investigated using laser heating of refractory materials. Three case studies using ^{27}Al in alumina nano-particles, ^{29}Si in silicon carbide and ^{23}Na in a glass-forming mixture of sodium carbonate and quartz have been conducted to distinguish the cases of (a) a fast-relaxing, high natural abundance nucleus, (b) a probe nucleus with low abundance and low spin-lattice relaxation rate, and (c) a complex and changing system of industrial relevance. The most suitable nucleus for *in-situ* high-temperature studies is one with high abundance but slow relaxation because the differential relaxation time between hot and cold parts of the sample effectively removes the signal from the cold material. There is no "*in-situ* penalty" from the diminishing Boltzmann polarisation at high temperature since this effect is balanced by a corresponding increase of the spin-lattice relaxation rate.

Introduction

A number of high-temperature NMR probes have been developed over the years [1, 2], but they have remained specialist instruments compared to liquids, magic-angle spinning (MAS), or field gradient (imaging) probes. The main reason for this lagging behind is the fact that, without MAS, solid-state NMR signals are broad and rather featureless and cannot easily be interpreted in the same way that liquid or MAS spectra can. The temperature range of the MAS technique is limited by the mechanical strength of zirconia rotors at elevated temperature, and MAS probe designs with gas stream, inductive, or laser heating [3, 4] were limited to about 530°C until recently. High-temperature MAS probes using a rotor encapsulated in a laser-absorbing sleeve have been developed more recently [5] and are now commercially available. Laser heating is superior to other techniques such as resistive or inductive heating in that it avoids electromagnetic interference. This enables temperatures beyond 2 000°C and containerless heating and aerodynamic levitation [6]. Most of these studies are concerned with the structure of melts and use mainly ^{27}Al [7–9] and occasionally ^{31}P [10] as a probe nucleus. The other main research strand is the dynamics of melts and glasses [11, 12], an area which has generated the earliest review of high-temperature NMR techniques [13]. A recent development is the use of pulsed gradients in a levitation experiment of a melt [14]. Aerodynamic levitation has also successfully been applied to x-ray and neutron scattering studies [15, 16]. Alternatively, laser heating has been applied to samples enclosed in boron nitride crucibles to study reactions between melts and solid grains [17, 18], including studies of ^{23}Na, ^{19}F and ^{17}O, and the batch melting process starting from solid raw materials [19]. Another advantage of laser heating is the fact that refractory materials can be studied under conditions resembling those they would encounter in practical use, *i.e.* steep temperature gradients and fast thermal cycling.

Materials and Methods

This laser-heated *in-situ* high-temperature NMR study entails three separate experiments aimed at investigating the limits of the technique. First, alumina nano-particles were chosen to determine the lower limit of detection of a liquid phase in the laser hot spot if a "good" NMR nucleus with high sensitivity and abundance and short relaxation time such as ^{27}Al is used. The second experiment is concerned with the time resolution achievable with a "moderate" NMR nucleus known for low natural abundance and long relaxation times such as ^{29}Si. Finally, results of an *in-situ* ^{23}Na NMR kinetic study of a solid-state reaction between sodium carbonate and quartz are shown as an example of what the technique can accomplish in a complex system of industrial relevance.

Laser-heated NMR probe design.

The laser-heated probe at UWA (cf. Fig. 1) is a specially commissioned probe design manufactured by Bruker. It is equipped with a 15 mm inner diameter horizontal saddle coil supported by a section of silica glass tube. Below the coil, a copper tube along the axis of the probe provides access for the laser beam. It can be sealed with a ZnSe window transparent to infrared radiation to allow air (or other gases) to be fed into the beam tube. The laser is a Synrad 125 W CO_2 laser operating at 10.6 μm wavelength, and is fed into the probe via a beam tube with a 90° mirror at the bottom of the magnet. The laser is aligned onto the sample position using a HeNe pointer laser collinear with the main laser. The beam can be focussed or broadened using a beam expander in the vertical beam tube. The

sample itself is mounted on a sample support machined from a BN rod. This can be a flat sample table with a small rim to keep the sample secured while inserting the probe into the magnet or a tapered tip for aerodynamic levitation. Samples can be self-supported powder pellets or powders enclosed in a BN container. The probe is operated inside a 9.4 T wide-bore cryomagnet. The ^{23}Na experiment was carried out on a similar system at CRMHT.

Fig. 2a shows a comparison of the ^{27}Al signal obtained at room temperature in the laser-heated probe and in a standard Bruker 4 mm MAS wide-bore probe (without spinning). The sample used in the laser probe on this occasion was a pellet of 4 mm diameter and 4 mm thickness. The flip angle was approximately 15 degrees in both cases, and a spectral width of 125 kHz was used. The line shape and line width is practically identical in both cases, although the signal-to-noise ratio of the MAS probe is better by a factor of 180. This is largely due to the wider coil diameter, which results in a much lower fill factor and r.f. field. Nevertheless, a decent quality ^{27}Al spectrum can be taken in less than 10 seconds. However, when the probe is used at high temperature for an extended period, the radio-frequency circuitry begins to heat up. The resulting change in the characteristics of the oscillating circuit causes a significant deterioration of the signal quality (cf. Fig. 2b), and it may be necessary to re-tune while at elevated temperature.

Temperature measurement and calibration.

A pyrometer is used to measure the temperature of a spot on the top of the sample. This requires a lens with a focal length of about 1 m because mounting the pyrometer head inside the bore of the magnet would dangerously restrict the heat flow away from the sample. The thermal gradient across a stationary (as opposed to levitated) refractory sample is considerable (cf. insert in Fig. 4); therefore the pyrometer reading must be regarded as a lower limit of the true sample temperature. In addition, in cases where a chemical reaction is followed in an *in-situ* experiment, the emissivity of the sample is bound to change, which will cause an additional error. Where a sample container is used, the most accurate temperature estimate is obtained by calibrating the laser output against a thermocouple tip placed in an empty sample container.

Results

^{27}Al NMR - Melting of refractory ceramics.

Heating a sample with a laser beam from one side produces steep thermal gradients. This form of heating allows us to study the structural response of refractory materials, which are designed specifically to cope with conditions such as thermal shock, $\frac{\mathrm{d}T}{\mathrm{d}t}$ and thermal gradients, $\frac{\mathrm{d}T}{\mathrm{d}x}$. The nature of NMR as a bulk technique, however, means that the signal obtained is an average of all environments in the sample. It is therefore important to judge the fraction of a phase that can be detected in a phase mixture.

Fig. 3 shows a high-temperature ^{27}Al NMR spectrum of alumina nano-particles. During the heat treatment, the particles agglomerate and subsequently sinter to form a dense refractory. The core of the specimen melts during this process as can be seen from the photographs shown in the insert in Fig. 3. As confirmed by MAS spectra, both the nano-particles and the product consist exclusively of octahedral aluminium sites near 0 ppm (relative to acidic $AlCl_3$ solution). On top of the broad line originating from the solid, a small narrow component can be made out near 60 ppm, which corresponds to motionally averaged tetrahedral sites in molten alumina. The line width of this peak

is 300-350 Hz, which is slightly wider than data obtained in [7] (200 Hz), indicating a small impurity contribution in this nano-phase material. The integral fraction of this peak in the spectrum shown is 3%. The lower limit of detection at the signal-to-noise ratio of these spectra is about 1%. These spectra were taken with 4000 averages with a 50 ms delay, giving a time resolution of 200 s. Since signal-to-noise goes with the square root of the number of averages, a 2% detection limit can be achieved with a time resolution of about 8 s.

^{29}Si NMR - Time resolution study.

^{27}Al is a rather benign NMR nucleus as long as very distinct environments such as tetrahedral *vs.* octahedral or solid *vs.* liquid are concerned. Its short relaxation time and high natural abundance ensure that good statistics can be obtained in an *in-situ* experiment with high time resolution. As a test case for a slow-relaxing nucleus, we have studied the ^{29}Si spectrum of SiC at high temperatures.

Fig. 4a shows ^{29}Si spectra taken in the laser probe at room temperature and at 1 480°C. The line near 110 ppm in the cold spectrum originates from the glass tube supporting the coil. The SiC line peaks near -20 ppm and covers all silicon sites in the different layers of the structure. These environments are rather similar, and MAS is needed to differentiate between them as the chemical shift of these sites ranges only from -14 ppm to -25 ppm [20]. The position of the line shifts slightly towards more negative chemical shift values. From thermal expansion alone, a shift in the opposite direction –if any– would be expected because the expansion of the lattice will reduce the electron density overall. Therefore, the polarity of the Si–C bond must be changing as the temperature rises, with electron density transferred from carbon atoms to silicon atoms.

It is remarkable that a very similar signal-to-noise ratio is obtained at both temperatures if the acquisition times are compared rather than the numbers of averages. The room temperature experiment uses 144 scans with a 5 s relaxation delay (9 min total acquisition time), while the hot experiment takes 5612 scans at 100 ms relaxation delay (12 min total acquisition time) to achieve a similar signal-to-noise ratio. The reduction in signal strength that is observed is due to the fact that the hot and cold parts of the sample have considerably different spin-lattice relaxation times. At the faster acquisition rate, cold material is saturated after just one or two pulses and does not contribute to the signal.

Fig. 4b explores the limit of time resolution for ^{29}Si, again taken as representative for a nucleus with rather low natural abundance and slow room-temperature relaxation. A signal-to-noise ratio of 3:1, limited to the hot fraction of the sample, can be achieved with about 900 scans, giving a time resolution of 90 s.

^{23}Na NMR - Glass forming kinetics.

As an example of the usefulness of laser-heated high-temperature NMR in complex materials of industrial relevance, we have studied the reaction of sodium carbonate and quartz below, at, and above the liquidus temperature of sodium disilicate, $Na_2Si_2O_5$ [19].

Fig. 5 shows a 2D plot of the ^{23}Na spectra obtained as a function of time. Each slice represents a spectrum averaged over one minute (128 averages with a delay of 460 ms). The third and last spectra are shown superimposed on the plot. There is a gradual movement of the median of the line from the sodium carbonate position at 1 ppm to that of sodium metasilicate, Na_2SiO_3, at 6 ppm. The metasilicate peak is significantly narrower than the sodium carbonate

peak of the original spectrum. The fact that the change in line position is gradual rather than a growth of a new component on top of the spectrum of the raw material suggests that the reaction progresses by sodium diffusion, a process during which the quartz grains are restructured to form metasilicate. Carrying out the experiment above the liquidus temperature of disilicate, the lowest-melting compound in the Na_2O–SiO_2 system, changes only the rate at which the reaction occurs but does not result in the detection of a liquid phase at any point. This indicates that sodium diffusion is sufficiently fast that the reaction front can pass through the region of the sample which is above the liquidus temperature without the formation of the equilibrium phase, *i.e.* disilicate melt.

In order to quantify the reaction kinetics it is necessary to deconvolve the spectra. Fig. 6 shows the five components used in fitting each slice of the *in-situ* high-temperature experiment. The system is too complicated to model the data with a quadrupolar line shape: Raw material and product line shape overlap to a large extent, and the lines are partially motionally narrowed. However, we do know the line positions of both the raw material and the product and can simulate the line shape empirically by overlapping Gaussians representing sodium carbonate and metasilicate and a contribution common to both to cover the quadrupolar tail of either line. It turns out [19] that this tail component does not vary very much with time and therefore does not produce a considerable error. In addition, a small fixed Gaussian contribution from the probe background is also included. From the fit results, the integral of the two main Gaussian lines represents the ratio of product and raw material (given that the tail component does not vary substantially) and can be taken as a reaction co-ordinate to describe the progress of the reaction. At all temperatures, the reaction kinetics appears to be saturating after a while, which is a more deceleratory behaviour than any of the standard models for diffusion-controlled growth predicts. This is caused by the thermal gradient within the sample, which results in a top layer which is not reactive on the time scale of the experiment.

Discussion

The objective of this study is to investigate the time resolution achievable in an *in-situ* NMR experiment using laser heating. From the three case studies it is clear that this depends on the relaxation time of the nucleus *at room temperature* and on the complexity of the spectrum, *i.e.* the number of different contributions to be separated and the extent to which their spectral features overlap.

As a general rule, the perfect nucleus for a high-temperature experiment will have high abundance (since enrichment is rarely justifiable in an experiment that is likely to evaporate a considerable fraction of the sample), low or no quadrupole moment (*i.e.* preferably $I = \frac{1}{2}$) and *long* spin-lattice relaxation time at room temperature. The slow relaxation rate will ensure that contributions from the cold parts of the sample are effectively removed from the spectra.

Boltzmann vs. relaxation.

Spin-lattice relaxation also compensates, for the most part, for any "*in-situ* penalty" resulting from the reduced Boltzmann polarisation at high temperature. The signal to be obtained from a transition between energy levels E_1 and E_2 is proportional to the Boltzmann polarisation

$$N_2 - N_1 \sim \exp\left(\frac{E_2}{k_B T}\right) - \exp\left(\frac{E_1}{k_B T}\right) \quad , \tag{1}$$

where $N_{1,2}$ are the respective populations, k_B is Boltzmann's constant, and T is the temperature. Therefore the signal obtained in a single scan is proportional to e^{-T}. At the same time, the spin-lattice relaxation rate increases following a similar Arrhenius-type law,

$$T_1^{-1} = \exp\left(-\frac{E_a}{k_B T}\right) \quad , \tag{2}$$

where E_a is the activation energy for the process that facilitates relaxation and T_1^{-1} is the spin-lattice relaxation rate. Since the relaxation delay needed to ensure that the sample is close enough to equilibrium before the next scan is proportional to the relaxation time (typically $5\,T_1$ is used), the number of scans that can be taken during a fixed period of time is also proportional to e^{-T}, just compensating for the loss in Boltzmann polarisation.

There are two limits to this mechanism, though. Fig. 7 shows ^{7}Li relaxation rate data of various forms of $LiTiS_2$ as an Arrhenius plot [21]. In this representation, the slope of the curve represents $-\frac{E_a}{k_B}$. It is clear from the graph that the Arrhenius relationship breaks down both at very low and very high temperatures. Only if spin-lattice relaxation is an activated process, *e.g.* if ionic motion or the creation of phonons is the mechanism that allows the energy from the NMR transition to be dissipated, the favourable temperature dependence is obtained. While low-energy mechanisms at the cold end of the temperature scale such as localised motion processes are not relevant here, the relaxation rate maximum is likely to be reached in some laser-heated *in-situ* experiments. This rate maximum is caused by a resonance of the Larmor frequency of the NMR transition and the frequency of the underlying relaxation process. If, for example, the activated relaxation process is ionic motion, then the rate maximum occurs at the temperature at which the hopping frequency of the ions matches the Larmor frequency of the spin system. This typically occurs near the melting point of a material because spin-lattice relaxation and structural relaxation are closely coupled processes. It must therefore be expected that the signal quality of a high-temperature NMR experiment will deteriorate near the melting point.

Outlook.

There are a number of improvements that can be made to laser-heated NMR probes that are used with static (as opposed to levitated) samples. The major concern is the removal of heat from the magnet bore above the coil and from the r.f. circuitry. This could be achieved by using a laminar flow of air on the inside of the probe's outer casing. This would also enable the existing axial air inlet to be used to supply reactive gases.

Another problem with high temperature measurements, particularly of reactive systems, is the accuracy of the temperature measurement, which is compromised by the changing emissivity of the sample. One option we have looked into is to use laser absorption radiation thermometry (LART) in conjunction with conventional pyrometry. LART uses two additional low-power infrared lasers at different wavelengths as a source of small surface temperature fluctuations, which are measured pyrometrically at these two wavelengths [22]. The results from the two measurements are divided by each other, and the emissivity cancels out of the equation. This technique is slow but could be used to re-calibrate the standard pyrometer dynamically.

Conclusions.

We have investigated the time resolution achievable in laser-heated *in-situ* high-temperature NMR experiments. For nuclei with high natural abundance and fast relaxation, a detection limit of 2% can easily be achieved with 3 s

resolution. However, the signal will contain contributions from both hot and cold parts of the sample, and only very distinct sites will be resolved at this rate. On the other hand, we were able to show that kinetics on a scale of minutes can successfully be investigated even in complex materials of industrial relevance. In slow-relaxing nuclei, the signal from any cold parts of the sample is effectively suppressed. Furthermore, the reduction of the signal accumulated per unit time due to the loss in Boltzmann polarisation at high temperature is compensated by the increase in the spin-lattice relaxation rate as long as the relaxation mechanism is thermally activated and the temperature is below the resonance of the Larmor frequency and the frequency of the underlying relaxation mechanism. The optimum nucleus for *in-situ* high-temperature studies is therefore an $I = \frac{1}{2}$ nucleus with high natural abundance and slow relaxation at room temperature.

Acknowledgements.
RW acknowledges funding from the UK Engineering and Physical Sciences Research Council and from Pilkington plc. For the ^{23}Na NMR experiment, access to the high-temperature NMR facility at CRMHT was granted under contract ARI HPRI-CT-1999-00042 from the European Union.

References

[1] Franke W., Heitjans P.: Ber. Bunsenges. Phys. Chem. **96**, 1674 (1992)
[2] Poplett I. J. F., Smith M. E., Strange J. H.: Meas. Sci. Technol. **11**, 1 703 (2000)
[3] Ferguson, D. B., Haw, J. F.: Anal. Chem. **67**, 3 342 (1995)
[4] Mldner, T., Ernst, H., Freude, D., Kärger, J., Winkler, U.: Magn. Reson. Chem. **37**, S 38 (1999)
[5] van Wüllen L., Schwering G., Naumann E., Jansen M.: Solid State Nucl. Magn. Reson. **26**, 84 (2004)
[6] Coutures. J. P., Massiot, D., Bessada, C., Echegut, P., Rifflet, J.-C., Taulelle. F.: C. R. Acad. Sci. Paris **310**, 1041 (1990)
[7] Poe, B. T., McMillan, P. F., Coté, B., Massiot, D., Coutures, J.-P.: J. Phys. Chem. **96**, 8 220 (1992)
[8] Poe, B. T., McMillan, P. F., Coté, B., Massiot, D., Coutures, J.-P.: J. Am. Ceram. Soc. **77**, 1 832 (1994)
[9] Florian P., Massiot D., Poe B., Farnan I., Coutures J. P.: Solid State Nucl. Magn. Reson. **5**, 233 (1995)
[10] Boucher, S., Piwowarczyk, J., Marzke, R. F., Takulapalli, B., Wolf, G. H., McMillan, P. F., Petuskey, W. T.: J. Eur. Ceram. Soc. **25**, 1 333 (2005)
[11] Böhmer, R., Diezemann, G., Hinze, G., Rössler, E.: Progr. Nucl. Magn. Reson. Spectr. **39**, 191 (2001)
[12] Ashbrook, S. E., Whittle, K. R., Le Polles, L., Farnan, I.: J. Am. Ceram. Soc. **88**, 1 575 (2005)
[13] Stebbins, J. F.: Chem. Rev. **91**, 1 353 (1991)
[14] Marzke R. F., Piwowarczyk J., McMillan P. F., Wolf G. H.: J. Eur. Ceram. Soc. **25**, 1 325 (2005)
[15] Landron C., Hennet L., Jenkins T. E., Greaves G. N., Coutures J. P., Soper A. K.: Phys. Rev. Lett. **86**, 4 839 (2001)
[16] Hennet L. *et al.*: Rev. Sci. Instrum. **77**, 05 3903 (2006)
[17] Robert, E., Lacassagne, V., Bessada, C., Massiot, D., Gilbert, B., Coutures, J.-P.: Inorg. Chem. **38**, 214 (1999)
[18] Lacassagne, V., Bessada, C., Florian, P., Bouvet, S., Ollivier, B., Coutures, J.-P., Massiot, D.: J. Phys. Chem. **B 106**, 1 862 (2002)
[19] Jones A. R., Winter R., Florian P., Massiot D.: J. Phys. Chem. **B 109**, 4 324 (2005)
[20] Guth J. R., Petuskey W. T.: J. Phys. Chem. **91**, 5 361 (1987)

[21] Winter R., Heitjans P.: J. Phys. Chem. **B 105**, 6 108 (2001)

[22] Levick A., Edwards G.: Anal. Sci. **17**, S 438 (2001)

Figure captions

Fig. 1: Coil section of the laser-heated NMR probe at UWA. The vertical saddle coil and supporting glass tube are at the centre. Below the base plate, the tune and match capacitors can be seen. A copper tube extending down to the base of the probe is used to feed cooling air and the laser beam into the coil section.

Fig. 2: a) Signal-to-noise of a typical static ^{27}Al NMR spectrum (of alumina nano-particles) at room temperature in the laser probe (grey) and in a standard (Bruker 4 mm wide-bore MAS) probe (black). b) Deterioration of signal quality after 30 min of heating at 30 W laser output (grey) due to heating of the r.f. circuitry compared to the original spectrum shortly after turning on the laser (black).

Fig. 3: Melting of Al_2O_3 nanoparticles. The insert shows samples after the experiment; the melted core is clearly visible in the third sample from the left.

Fig. 4: a) Spectra of SiC taken in the high-temperature probe at room temperature (black) and at 1480°C(grey). The line near -110 ppm originates from the glass coil support. b) Maximum time resolution achievable for ^{29}Si at natural abundance in an *in-situ* experiment. The black spectrum was averaged over 9 min, the grey one over just 90 s. The insert shows the top and bottom faces of a sample after heat treatment.

Fig. 5: Evolution of *in-situ* ^{23}Na spectra of a glass-forming batch at 855°C with time (evolving from bottom to top). Each horizontal slice is averaged over a 1 min period. The shades of grey represent amplitudes. Spectra taken after 3 min and after 80 min, corresponding to the bottom and top slices in the two-dimensional plot in the background, are superimposed [19].

Fig. 6: Deconvolution of a wide-line high-temperature spectrum. The four Gaussian components relate to the product (Na_2SiO_3), raw material (Na_2CO_3), probe background, and quadrupolar tail (peak maxima from left to right) [19].

Fig. 7: Arrhenius plots of the spin-lattice relaxation rate *vs.* inverse temperature of amorphous (a), nano-crystalline (n2), and macro-crystalline (h) Li_xTiS_2. Relaxation in these systems is facilitated by mobile Li^+ ions; the slope of the curve corresponds to the activation energy of short-range ionic motion [21].

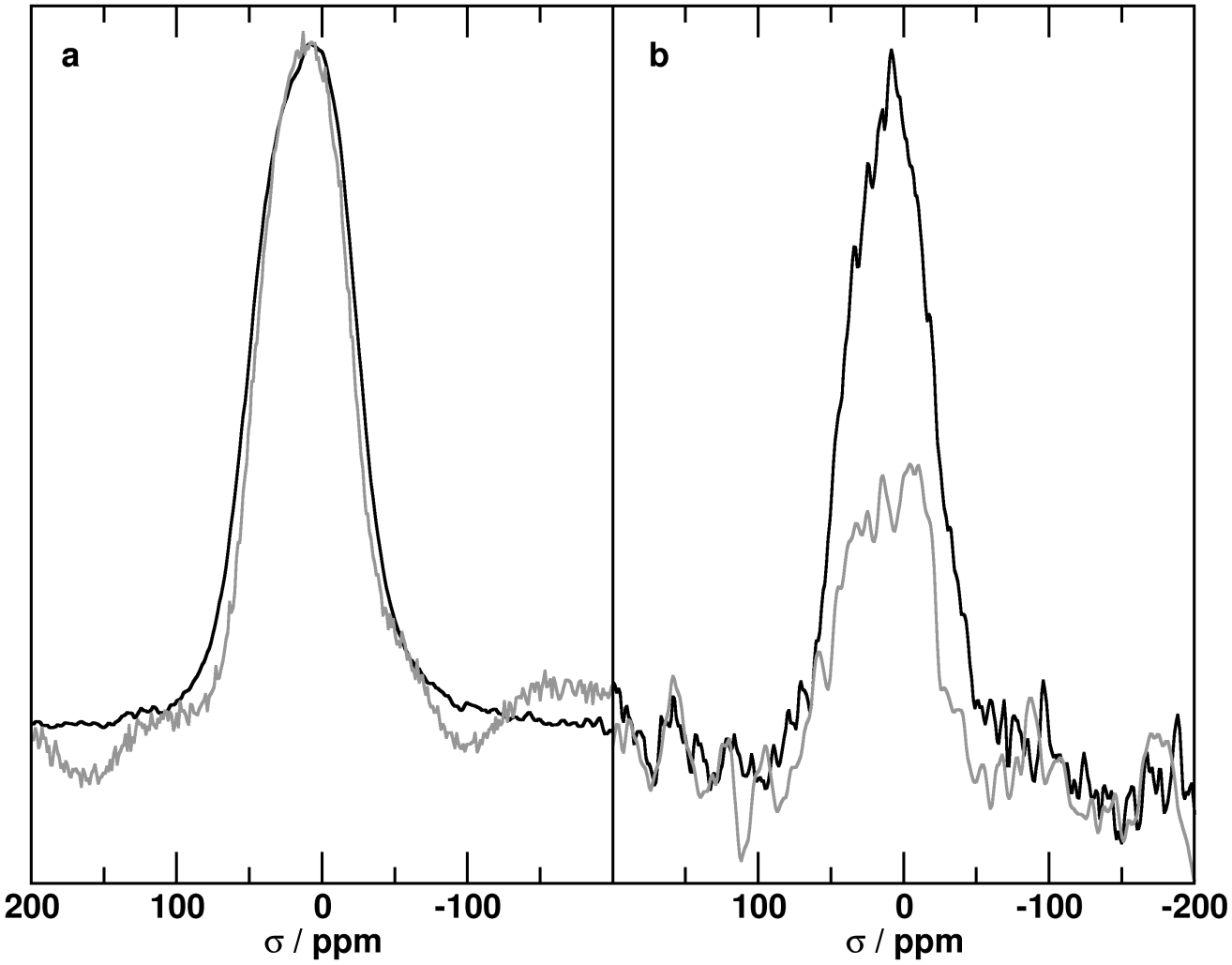
a
b
200
100
0
-100
σ / ppm
100
0
-100
-200
σ / ppm

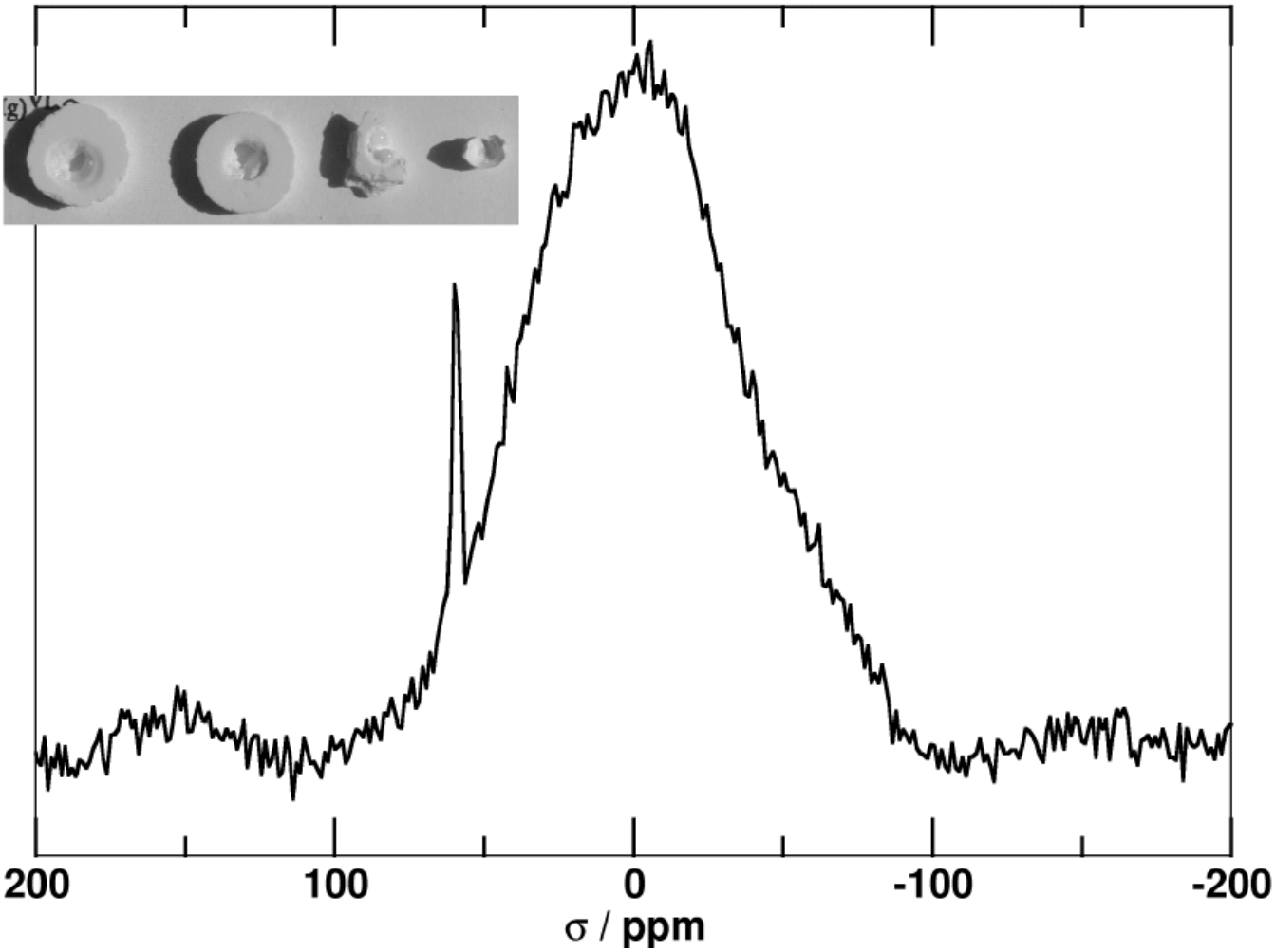
200
100
0
-100
-200
σ / ppm

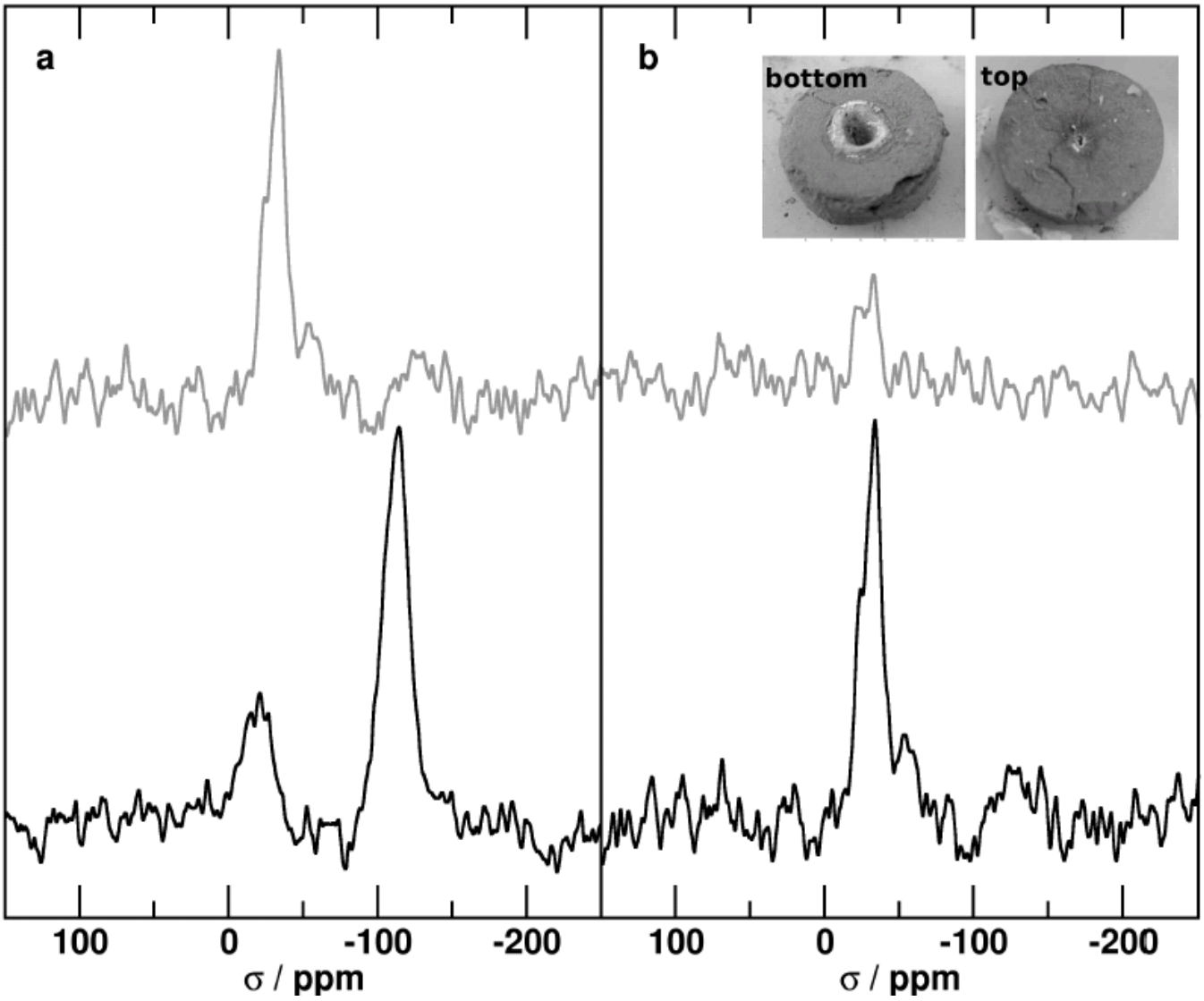
a
b
bottom
top
100
0
-100
-200
σ / ppm
100
0
-100
-200
σ / ppm

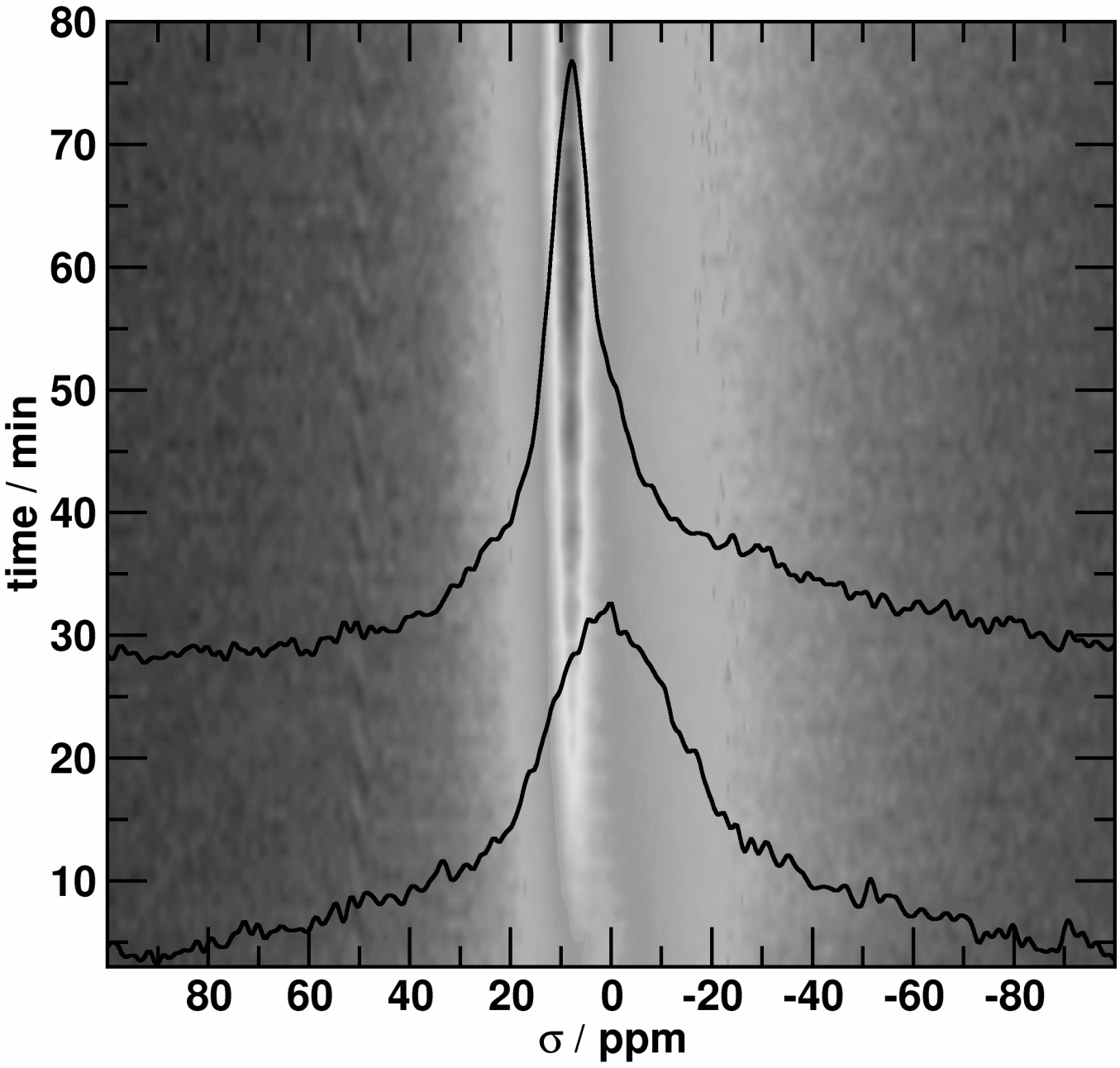
80
70
60
50
40
30
20
10
time / min
80
60
40
20
0
-20
-40
-60
-80
σ / ppm

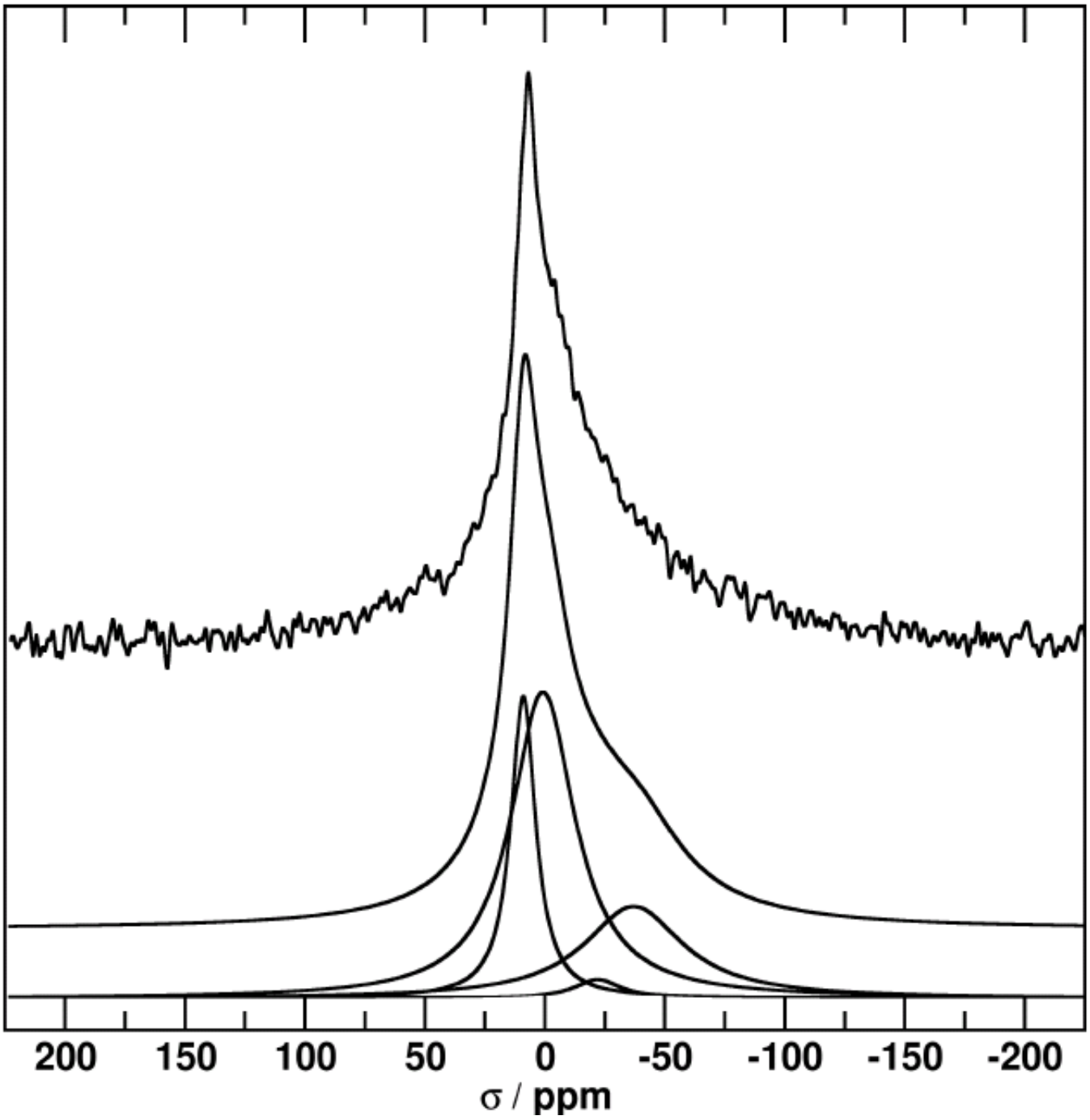
200
150
100
50
0
-50
-100
-150
-200
σ / ppm

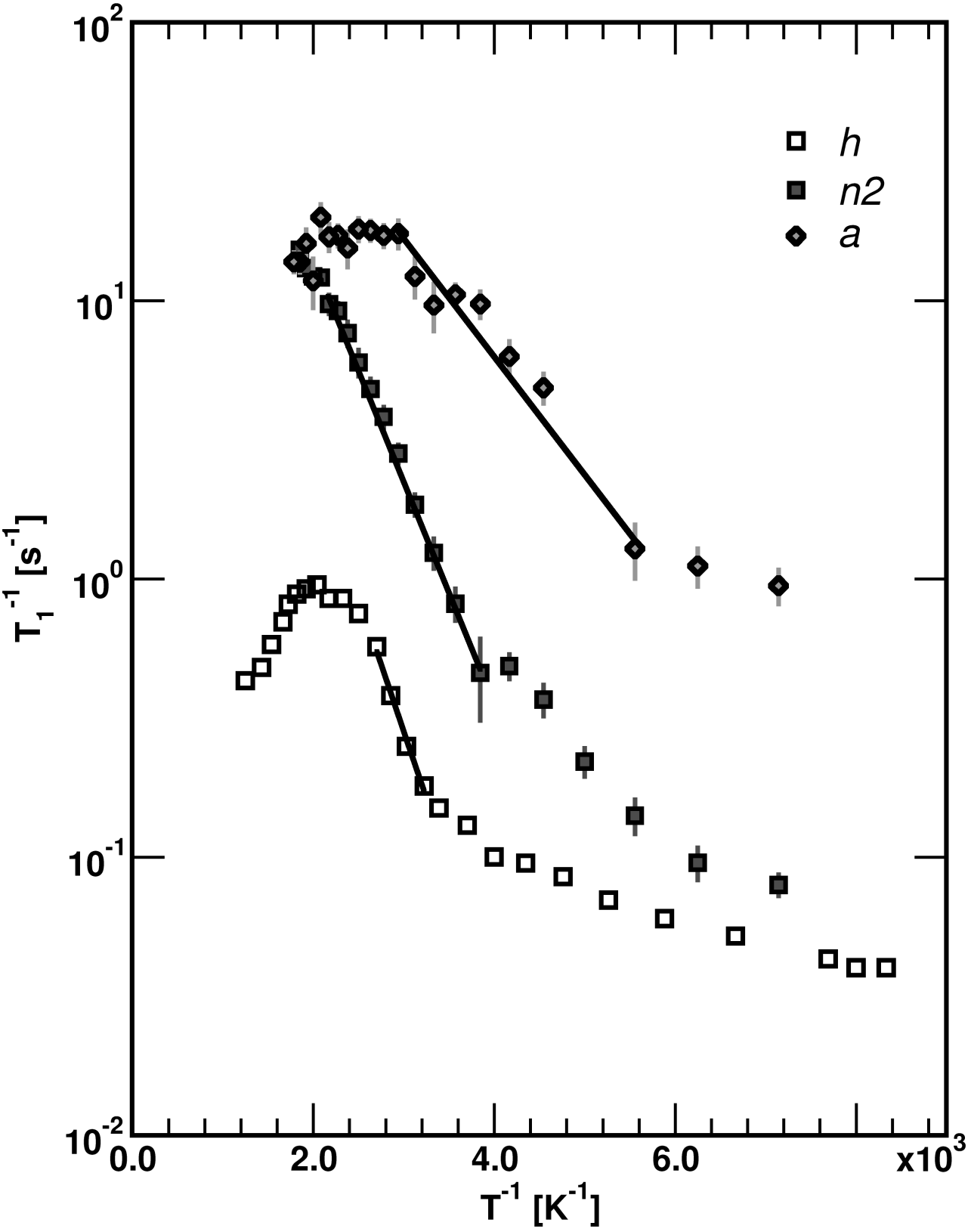
h
n2
a
10^2
10^1
10^0
10^{-1}
10^{-2}
T_1^{-1} [s^{-1}]
0.0
2.0
4.0
6.0
x10^3
T^{-1} [K^{-1}]

rw/070503